Review

Cardiovascular MRI for the Assessment of Heart Failure: Focus on Clinical Management and Prognosis

Stefano Muzzarelli, MD,[1,2]* Karen Ordovas, MD,[1] and Charles B. Higgins, MD[1]

Cardiovascular MR (CMR) has an emerging role in the noninvasive diagnostic assessment of heart failure (HF). Different imaging sequences allow for a detailed assessment of cardiac morphology, function, myocardial perfusion, tissue characterization, and blood flow measurement. This article reviews the key applications of CMR in HF, with special focus on how CMR may influence the diagnostic and therapeutic approach of HF patients.

Key Words: MRI; heart failure; diagnosis; prognosis; patient management
J. Magn. Reson. Imaging 2011;33:275–286.

MULTIPLE CARDIAC IMAGING modalities are used for the assessment of patients with heart failure (HF). The major clinical questions to be answered for a comprehensive evaluation of HF patients include the following: (i) precise definition of ventricular size and function, (ii) identification of the cause of HF, (iii) determination of myocardial viability, (iv) assessment of myocardial perfusion, (v) evaluation of mechanical dyssynchrony, and (vi) exclusion of pericardial diseases potentially mimicking HF. Cardiovascular MR (CMR) has emerged as a pivotal technique in the arena of cardiovascular imaging as an alternative, complementary, and frequently superior imaging modality, allowing for a comprehensive evaluation of all the above mentioned clinically relevant issues. This review addresses the role of CMR for the assessment of patients with HF, highlighting advantages and limitations compared to other imaging modalities and focusing on the role of CMR for guiding therapeutic approaches.

[1]Department of Radiology, University of California, San Francisco, California, USA.
[2]Department of Cardiology, University Hospital Basel, Basel, Switzerland.
Contract grant sponsor: Swiss National Science Foundation; Contract grant number: PBBSP3-125579, Berne, Switzerland.
*Address reprint requests to: S.M., University of California, San Francisco, Department of Radiology, Box 0628, 505 Parnassus Avenue, Room M-396, San Francisco, CA 94143-0628. E-mail: muzzarellis@uhbs.ch
Received May 3, 2010; Accepted October 20, 2010.
DOI 10.1002/jmri.22433
View this article online at wileyonlinelibrary.com.

CMR FOR QUANTIFICATION OF VENTRICULAR VOLUMES AND SYSTOLIC FUNCTION

Precise quantification of the ventricular volumes and systolic function is of great clinical relevance. Indeed, these parameters are major determinants of prognosis and clinical decision making in patients with HF, because the indication for internal cardioverter defibrillator (ICD), cardiac resynchronization therapy (CRT), valve replacement therapy, and specific HF drugs is dependent on left ventricular ejection fraction (LVEF) and size (1–4). Therefore, an accurate and reproducible quantification of LVEF is required for appropriate risk stratification and treatment allocation of patients. There is a growing body of evidence that right ventricular (RV) function also is a powerful predictor of survival in HF patients, supporting the importance of accurate measurement of RV function in HF patients (5,6).

Currently, breathhold ECG gated cine steady-state free precession (SSFP) is preferred to the spoiled gradient echo sequence for the acquisition of cine loops. This approach achieves better signal-to-noise, contrast-to-noise, higher temporal resolution and better definition of the endocardial border (7,8). The excellent image quality generated by SSFP pulse sequences allows for highly reproducible measurements, so that CMR is now recognized as the gold standard method for the quantification of left ventricular (LV) and RV volumes and systolic function (9). Normal range of LV and RV ejection fraction and dimensions as assessed with SSFP cine imaging has been previously described (10,11). The ability to obtain images in all plane directions, good temporal and spatial resolutions, reliable endocardial border detection, and the independency of geometrical assumptions for the quantification of the ventricular volumes, are main advantages of CMR compared to other imaging modalities. This is particularly true for the assessment of the RV volumes, where echocardiography is strongly limited by the complexity of the ventricular geometry.

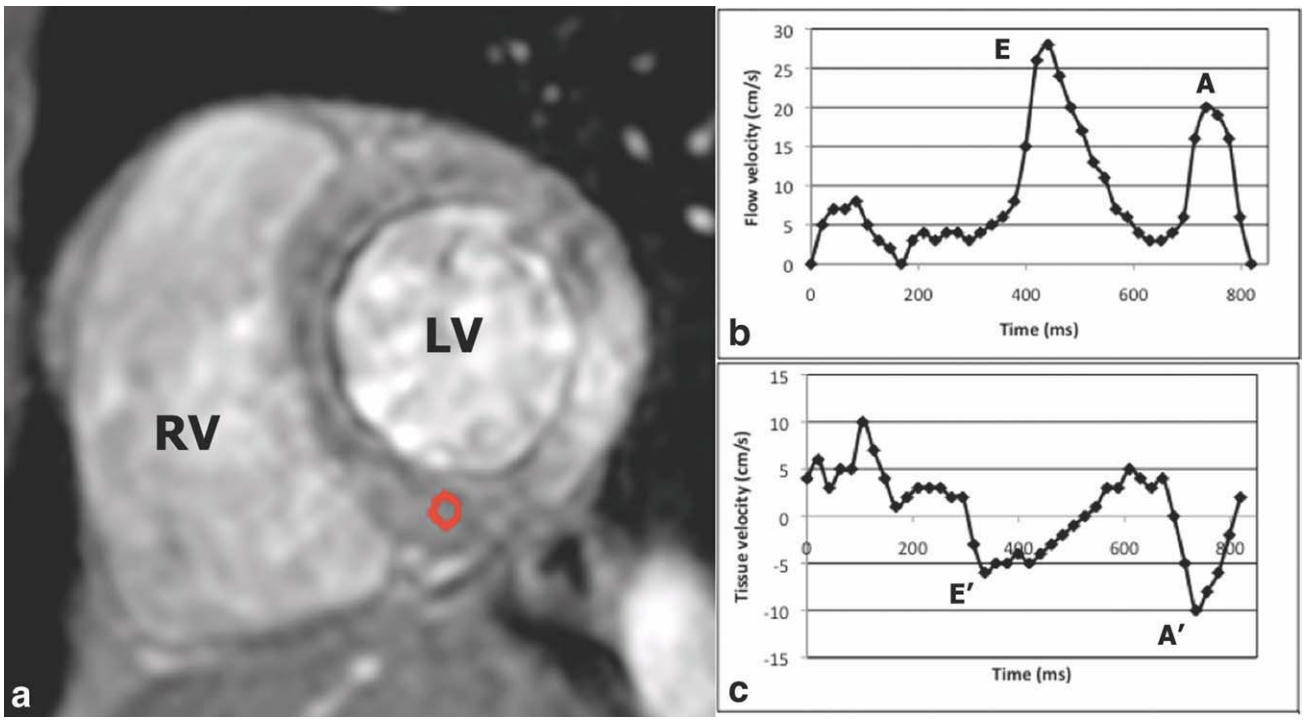

Figure 1. Assessment of diastolic function by velocity-encoded cine imaging. **a**: Magnitude image of velocity-encoded cine sequence showing the preferred location for the measurement of tissue velocity at the basal portion of the infero-septal LV myocardium. **b**: Transmitral flow curve shows early (E) and late (A) diastolic inflow peaks, reflecting passive and active left ventricular filling. **c**: Myocardial longitudinal velocity curve is shown. The first (E′) diastolic tissue velocity peak reflects early myocardial relaxation and the second reflects late (A′) diastolic relaxation. LV, left ventricle; RV, right ventricle.

CMR FOR THE ASSESSMENT OF DIASTOLIC FUNCTION

Up to 50% of patients with symptomatic HF have a preserved LV ejection fraction (HFPEF) and diastolic dysfunction is, therefore, the primary cause of HF in such patients (12). Recent studies suggest that these HF patients have similar prognosis to those with reduced ejection fraction (13). From the pathophysiologic point of view, HFPEF is caused by impaired ventricular relaxation and increased ventricular stiffness, leading to increased cardiac filling pressures. Recently, new diagnostic criteria of HFPEF have been published (12). If diastolic dysfunction is present in patients with reduced LVEF, it is also associated with a worse prognosis (14). Evaluation of diastolic function is, therefore, important for the assessment of HF patients.

Echocardiography has been widely studied and validated for the assessment of the diastolic LV function and represents the preferred modality for the noninvasive assessment of diastolic function. Nevertheless, recent developments show the potentiality of CMR for the quantification of diastolic function. Estimation of the ratio between the peak early mitral inflow velocity (E) divided by the early diastolic longitudinal lengthening velocity of the LV basis (E′) has been shown to correlate with the LV end-diastolic pressure and is the most robust echocardiographic parameter for estimating LV filling pressures. A ratio $E/E' < 8$ is considered normal, $E/E' > 15$ is consistent with elevated LV filling pressures, and finally, E/E′ between 8 and 15 is suggestive but nondiagnostic evidence of diastolic LV dysfunction (12). In echocardiography, E and E′ is obtained using flow- and tissue-velocity Doppler imaging (12). Similarly, a CMR technique based on velocity-encoded cine imaging can quantify mitral diastolic flow (E) and diastolic longitudinal myocardial lengthening velocity of the LV basis (E′; Fig. 1). Prior studies have indicated a tight correlation between CMR and echocardiography-derived E/E′ as well as invasively measured filling pressures (15,16). However, the measurement of the mitral diastolic flow by two-dimensional velocity-encoded cine imaging may be inaccurate if the interrogation plane is off-axis of the flow direction and if a sequence with insufficient temporal resolution is used. In addition to the above-mentioned method based on flow and tissue velocity, other CMR techniques based on myocardial tagging have been described (17,18). However, because guidelines for the definition of HFPEF and the prognostic data are mainly based on E/E′ by echocardiography, this method remains the preferred in clinical practice (12,14).

CMR TO IDENTIFY THE CAUSE OF HF

Prognosis and treatment of patients with HF differs considerably depending on the underlying cause. Identification of patients with coronary artery disease (CAD) is highly relevant, because CAD is associated with a worse prognosis (19). In addition, patients with CAD may benefit from coronary revascularization and secondary preventive measures (2). Patients without

evidence of CAD may have a broad spectrum of possible etiologies, including genetic, mixed, or acquired forms of cardiomyopathy (CMP; 20). Because some forms of nonischemic CMP, such as cardiac sarcoidosis or Anderson-Fabry disease, may be cured with specific treatments, accurate diagnosis is important. Additionally, if a genetic CMP is suspected, family screening may become important for early diagnosis.

Traditionally, coronary angiography is performed for the identification of those patients with CAD, while the diagnosis of nonischemic CMP is made in those patients without obstructive CAD. As discussed in more detail in the next section, CMR with delayed gadolinium enhancement (DGE) has emerged as an alternative method for differentiating between ischemic and nonischemic CMP in the setting of HF (21). Additionally, T2* imaging may be used to measure the myocardial iron concentration, establishing the diagnosis of rare cardiac pathologies related to myocardial iron accumulation in the setting of posttransfusional siderosis, hemochromatosis, or siderosis related to liver disease (22,23). Furthermore, T2-weighted sequences can be used for the detection of myocardial edema. Before discussing clinical applications, a brief overview about the general principles of DGE, T2* and T2-weighted imaging will be provided.

Imaging Techniques for Characterizing Cardiomyopathies

Delayed Gadolinium Enhancement Imaging

The gadolinium hyperenhancement of myocardial necrosis and fibrosis is based on the following principles: (i) Gadolinium chelates are extracellular contrast agents, which are not able to cross an intact cellular membrane (24). (ii) In acute myocardial necrosis, the myocardial cellular membranes are disrupted, dysfunctional and, therefore, permeable to gadolinium. In areas of chronic myocardial infarction (MI) or fibrosis, myocardial cells are replaced by extracellular collagen matrix. Therefore, the distribution volume of gadolinium is increased in both acute and chronic MI (25). (iii) Additionally, the kinetics of contrast enhancement is characterized by a delayed wash-out of gadolinium in infarcted compared to normal myocardium (26). These principles explain why areas of fibrosis or necrosis have higher signal intensity compared to normal myocardium on delayed T1-weighted CMR sequences after administration of gadolinium. Animal studies confirmed that DGE imaging allows for reliable and precise localization and quantification of MI (27). Inversion recovery (IR) sequences with inversion time set to null the signal of normal myocardium are used to maximize the contrast between normal myocardium and areas of enhancement (28). Further developments have shown advantages of phase-sensitive IR sequences for determination of the infarct size (29).

T2-Star Imaging

Iron is a molecule with ferromagnetic characteristics. Therefore, deposition of iron in the myocardium leads to shortening of the T2-Star (T2*) relaxation time because of enhanced inhomogeneity in the local magnetic field. Because relaxometry CMR is able to measure the T2* value of a tissue of interest, estimation of the tissue iron concentration may be derived. Recently, black-blood T2* techniques have been shown to improve accuracy and reproducibility of myocardial T2* measurements (30).

T2-Weighted Imaging

Cardiac T2-weighted imaging is aimed at detecting edema of the myocardial tissue. Triple-inversion recovery spin echo with fat saturation "black-blood" images are usually used for cardiac T2-weighted imaging (31). A recent report revealed the advantages of a combined hybrid sequence between steady-state free precession and turbo spin echo for bright blood T2-weighted myocardial imaging; this sequence can overcome the issue of residual bright rim artifacts next to the endocardium due to inadequate suppression of the blood pool signal on spin echo images (32). Importantly, this sequence should be performed before gadolinium administration, because gadolinium also changes T2-relaxation.

Clinical Application of DGE, T2, and T2-Weighted Imaging for the Determination of the Cause of HF*

Several mechanisms may cause LV dysfunction in patients with CAD, including the following: (i) myocardial scar tissue, (ii) myocardial stunning, (iii) hibernating myocardium, and (iv) negative remodeling process. Myocardial stunning is a reversible myocardial contractile abnormality caused by single or repetitive *brief episodes* of myocardial ischemia. Hibernating myocardium is caused by a *persistent* hypoperfusion, which is not severe enough to cause myocardial cell death, but is sufficient to cause contractile dysfunction (33). Both forms are reversible after restoration of myocardial perfusion, but weeks may ensue before functional recovery occurs (34). Postinfarction remodeling is a process characterized by a progressive maladaptation of the myocardial tissue after myocardial injury, consisting of fibrosis, apoptosis and myocyte hypertrophy. This remodeling process is mainly driven by overstimulation of the neuroendocrine system and contributes to progressive ventricular wall thinning, dilation, and functional compromise even in noninfarcted myocardium (35).

Myocardial scar imaging with DGE can identify an ischemic etiology in patients with HF. Based on the pathophysiology of MI, patients with CAD are expected to have subendocardial or transmural myocardial scar tissue, with a distribution area corresponding to the vascular bed of an epicardial coronary artery (Fig. 2). Conversely, patients with nonischemic CMP may have no detectable fibrosis or myocardial fibrosis without mural or segmental localization characteristic for CAD (i.e., midwall, subepicardial location, patchy distribution; 21). Therefore, the presence, the extent and the localization of DGE may distinguish LV dysfunction related to ischemic versus

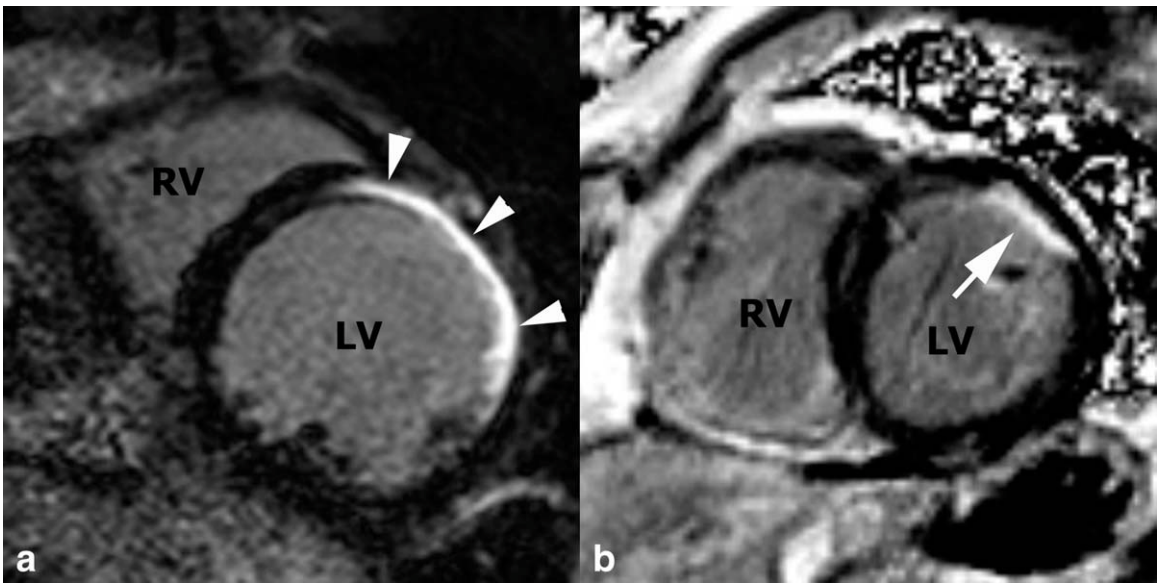

Figure 2. Myocardial infarction. Delayed gadolinium enhancement short axis image showing examples of (**a**) transmural (arrowheads), and (**b**) nontransmural subendocardial myocardial infarction (arrow). LV, left ventricle; RV, right ventricle.

nonischemic CMP. Moreover, specific patterns of DGE may be suggestive for some forms of nonischemic CMP such as sarcoidosis (Fig. 3), Anderson-Fabry disease, hypertrophic CMP (Fig. 4), cardiac amyloidosis (Fig. 5), or myocarditis (Fig. 6; 36–39). The typical patterns of DGE in ischemic and nonischemic CMP are schematically shown in Figure 7.

In a comparative study of DGE-CMR and coronary angiography in 90 patients with HF and reduced LVEF, 30% had documented obstructive coronary lesions, while 70% had unobstructed coronary arteries (40). All patients with angiographic evidence of CAD showed DGE with a typical distribution for CAD, providing 100% sensitivity for detection of CAD. Among patients without angiographic evidence of CAD, there were three different findings: 59% had no DGE, 28% had patchy or longitudinal striae of midwall DGE, and 13% had DGE, which was indistinguishable from patients with CAD. The interpretation of DGE with a CAD pattern in patients without evidence of obstructive CAD is uncertain but may reflect a prior MI with recanalization of the culprit coronary vessel. Thus, these authors suggested that coronary angiography alone may lead to diagnostic

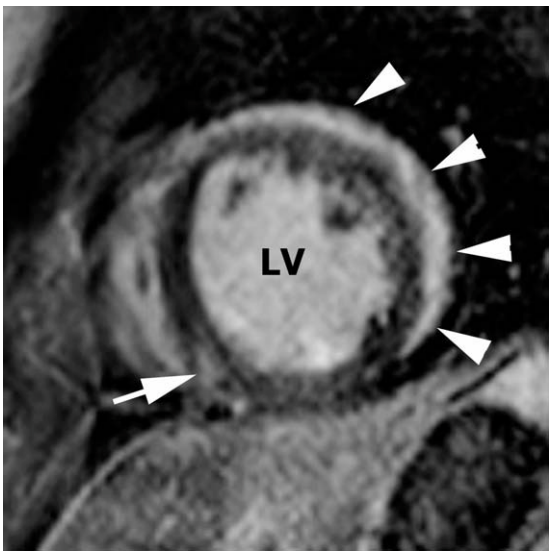

Figure 3. Cardiac sarcoidosis. Delayed gadolinium enhancement short axis image showing an extensive subepicardial hyperenhancement of the anterior, anterolateral, and inferolateral wall (arrowheads). An involvement of the posterior hinge point is noted (arrow). LV, left ventricle.

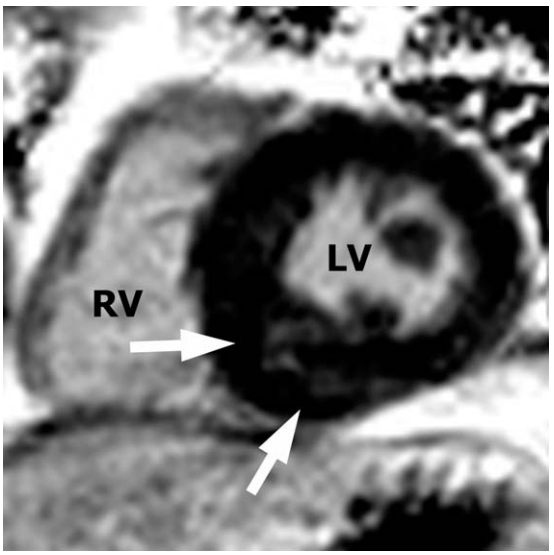

Figure 4. Hypertrophic cardiomyopathy. Delayed gadolinium enhancement short axis image showing septal myocardial hypertrophy with multiple focal, and partially confluent areas of hyperenhancement (arrows). LV, left ventricle; RV, right ventricle.

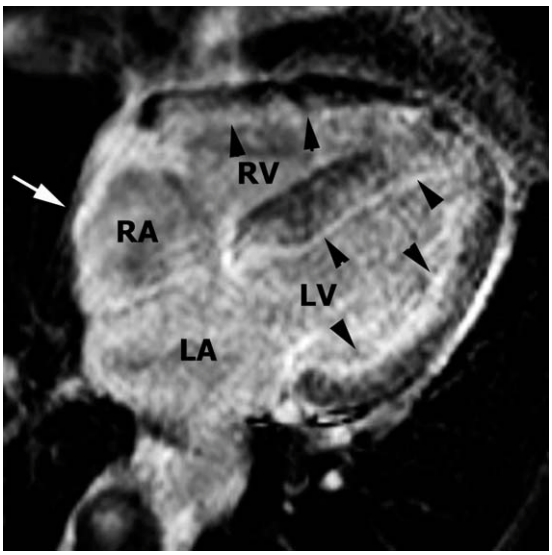

Figure 5. Cardiac amyloidosis. Delayed gadolinium enhancement horizontal long axis image demonstrating global subendocardial hyperenhancement of the thickened myocardium of both ventricles (arrowheads), and hyperenhancement of the thickened atrial myocardium (arrow), typical presentation of cardiac amyloidosis. LV, left ventricle; RV, right ventricle; LA, left atrium; RA, right atrium.

misclassification regarding the cause of HF in some patients (40). Other studies have also confirmed a high accuracy of CMR for detecting CAD in HF patients. However, absence of DGE or DGE without CAD distribution has been described in up to 15% of patients with documented CAD (41–43). Possible explanations of this finding includes the following: (i) presence of a concomitant myocardial disease (i.e., alcoholic CMP) other than CAD, causing systolic LV dysfunction; (ii) presence of extensive collaterals causing a DGE pattern other than subendocardial or transmural in cases of MI; and (iii) LV systolic dysfunction caused by repeated stunning or hibernation in absence of prior MI.

As discussed above, T2* imaging may be implemented to diagnose iron overload CMP, follow-up the therapeutic effects of iron-binding therapy, and provide cardiac risk stratification in such patients. A T2* value of >20 ms (usually >40 ms) is considered normal, between 10 ms and 20 ms moderately abnormal, and <10 ms severely abnormal (44–46). HF caused by myocardial iron deposition such as in thalassemia is invariably associated with a T2* < 10 ms.

T2-weighted imaging identifies myocardial edema. This application has been shown to increase the diagnostic accuracy of CMR compared to DGE alone in patients with suspected acute myocarditis, which is one of the potential causes of acute HF, and also has the potential to detect myocardial edema related to heart transplant rejection (47–49).

CMR may be an alternative method to routine coronary angiography for a noninvasive diagnostic work-up of patients with HF. The ability of CMR for detecting even small subendocardial MIs and the capability for other types of myocardial tissue characterization are major advantages of CMR compared to other imaging techniques in HF patients. In a comparative study between DGE-CMR and myocardial perfusion single photon emission computed tomography (SPECT; MPS) Wagner et al showed that small or subendocardial MIs may be missed by MPS due to the lower spatial resolution of MPS (in-plane resolution of 10 × 10 mm) compared with DGE-CMR (in-plane resolution of 1.4 × 1.9 mm; 50). Specifically, all segments with nearly transmural MI, as defined by DGE-CMR, were detected also by MPS. On the other hand, nearly half of the segments with subendocardial MI were missed by MPS (50).

CMR FOR PATIENT SELECTION TO REVASCULARIZATION PROCEDURES

Viability

Reversibility of chronic LV dysfunction is an important clinical consideration in patients with CAD. Revascularization of viable myocardium leads to improvement of LV function, HF symptoms, and survival (51). In this context, the identification of viable myocardium is of utmost importance for targeting myocardial revascularization procedures in patients with CAD and reduced LV function. Dysfunctional but viable myocardium consists of myocardial tissue containing vital myocardial cells with reduced mechanical contractile function due to hypoperfusion (hibernation or repetitive stunning). The assessment of myocardial viability may rely either on morphological parameters, such as demonstration of scar or alternatively on functional parameters, such as myocardial metabolic activity or contractile reserve in response to an inotropic agent (52).

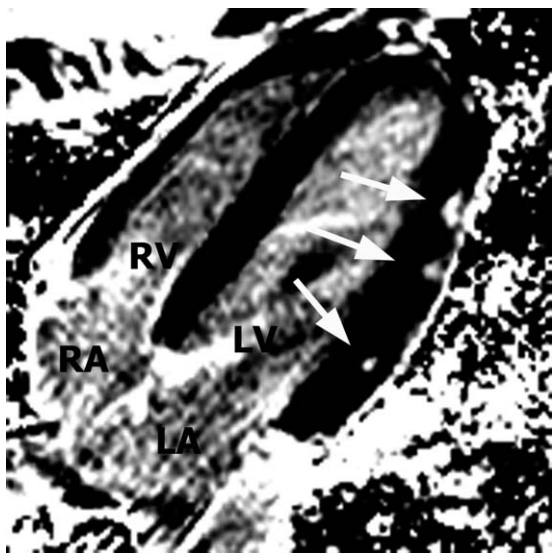

Figure 6. Myocarditis. Delayed gadolinium enhancement horizontal long axis image demonstrating multiple foci of midmyocardial and subepicardial hyperenhancement, which is a typical finding of myocarditis (arrows). LV, left ventricle; RV, right ventricle; LA, left atrium; RA, right atrium. (Courtesy of M.J. Zellweger, University Hospital Basel, Switzerland).

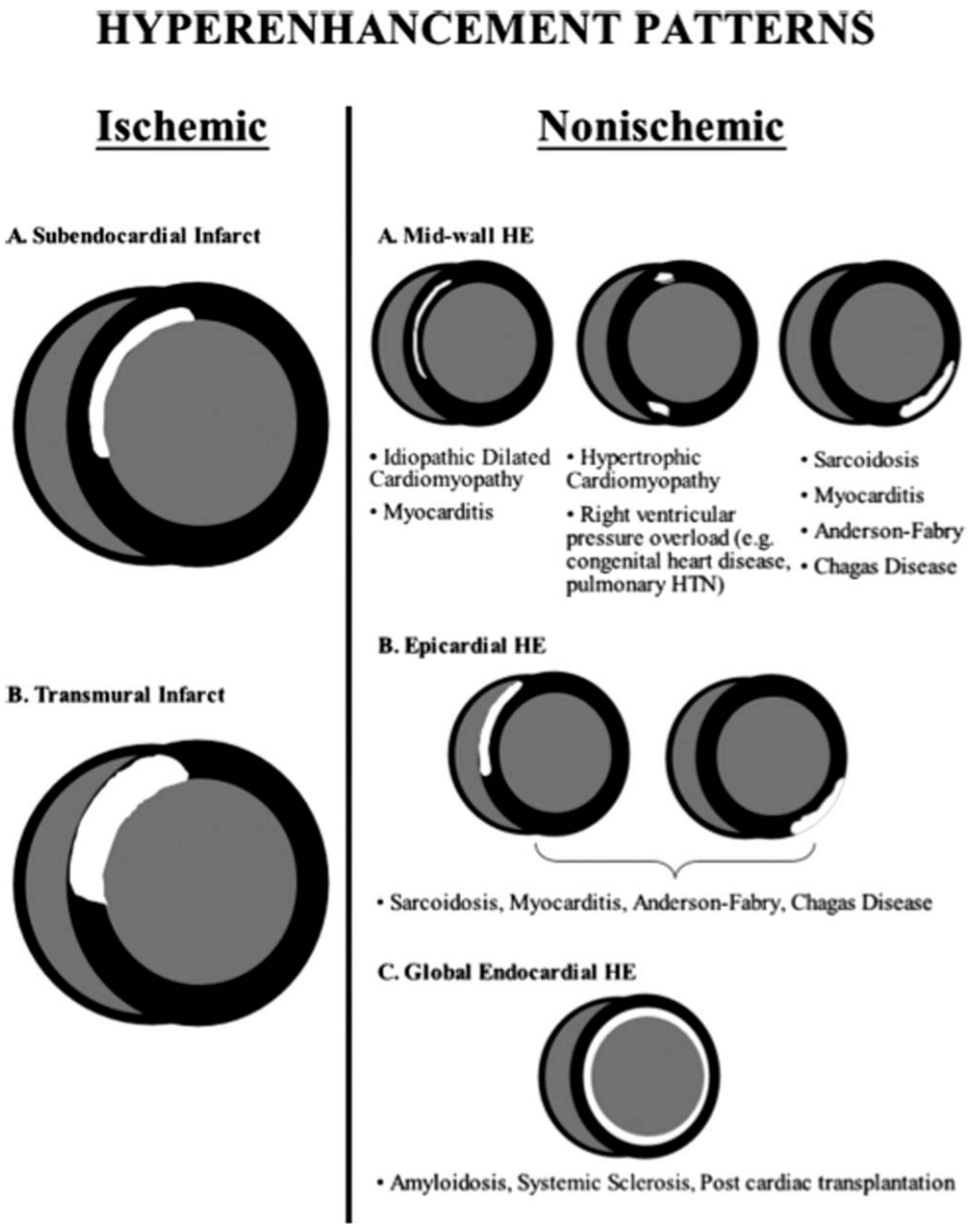

Figure 7. Hyperenhancement patterns in ischemic and nonischemic cardiomyopathy. In ischemic cardiomyopathy, hyperenhancement is subendocardial or transmural, with a distribution corresponding to the vascular bed of an epicardial coronary artery. Other forms of hyperenhancement patterns suggest a nonischemic cardiomyopathy. Reprinted by permission from Mahrholdt et al (21).

CMR BASED ASSESSMENT OF MYOCARDIAL VIABILITY

Transmural Extent of DGE

The functional recovery after revascularization is inversely proportional to the transmural extent of MI (Fig. 2). CMR-DGE viability assessment has been shown to predict segmental functional recovery after reperfusion of acute MI and after revascularization for chronic CAD (53–56). Studies performed on patients with chronic CAD showed consistently that in segments without evidence of scar (no CMR-DGE) the chance of recovery was 75–80%. In contrast, the chance of recovery decreased to 60%, 40%, less than 20%, and finally 1–3% as transmural extent of DGE increased in quartiles from 1–25%, 26–50%, 51–75%, and 76–100%, respectively (55,56). In addition to the transmural extent of DGE, the absolute thickness of the viable myocardium is important for predicting functional recovery after revascularization, because a minimal amount of contractile myocardium is required to produce enough power to overcome intramyocardial wall tension, which in turn is related to the ventricular radial dimension and to the myocardial wall thickness. Cutoff values for minimal thickness of nonenhanced myocardium of 4.5 mm to 5.1 mm in chronic MI have been reported for functional recovery after revascularization (57,58).

Microvascular Obstruction

The phenomenon of microvascular obstruction (MVO) is defined as a failure of myocardial tissue reperfusion in the core zone of the MI, despite successful recanalization of the occluded epicardial coronary artery (no-reflow), as a consequence of capillaries compression due to myocardial edema, capillary occlusion with microthrombotic material, or capillary necrosis (59). This pathophysiological background is important for understanding the association between MVO and

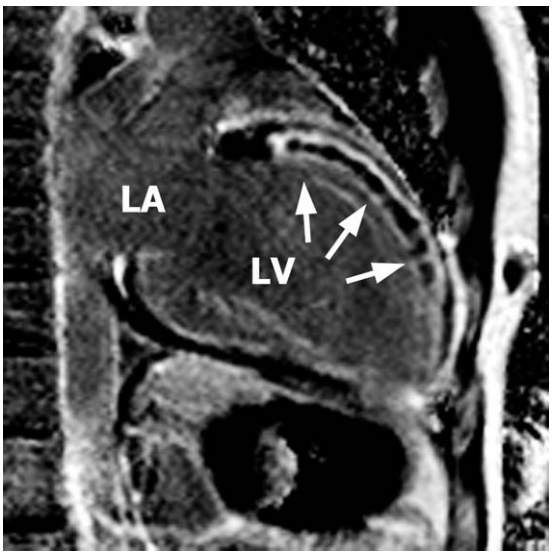

Figure 8. Microvascular obstruction. Delayed gadolinium enhancement vertical long axis image demonstrating microvascular obstruction of the anterior LV myocardium, characterized by a central nonenhanced zone (zone of no-reflow) surrounded by hyperenhanced myocardium (arrows). LV, left ventricle; LA, left atrium.

absence of viability. First-pass perfusion CMR imaging, showing hypoenhancement during the first pass of gadolinium, as well as DGE showing areas of dark, nonenhanced zones surrounded by hyperenhanced myocardium (Fig. 8), enable identifying MVO in acute MI (60). The identification of MVO as assessed with CMR has been shown to be a strong and independent predictor of nonviability, adverse myocardial remodeling and major adverse cardiovascular events after acute MI (60–62).

Contractile reserve

Low-dose dobutamine stress CMR may be implemented for assessing contractile reserve of dysfunctional segments as an indicator of tissue viability. Advantages of this technique for predicting functional recovery compared to DGE viability assessment have been reported in patients with intermediate transmural extent of DGE. This was shown by Wellnhofer et al demonstrating that in segments with 1–74% DGE transmurality, accuracy of predicting functional recovery after revascularization is improved by additional evaluation of contractile reserve in response to low-dose dobutamine (63).

B) Perfusion

Multiple studies have confirmed a high diagnostic accuracy and safety of first-pass gadolinium CMR perfusion imaging with vasodilator stress for detection of hemodynamic relevant CAD, reaching a sensitivity of 91% and a specificity of 81% in a pooled meta-analysis (64). Recent comparative studies suggest that the diagnostic accuracy of perfusion CMR is equal or superior compared to myocardial perfusion SPECT and positron emission tomography (65,66). However, perfusion CMR is still not widely used in clinical practice.

The severity of myocardial ischemia is a powerful outcome predictor in patients with CAD and there is rising evidence that the benefit of revascularization among patients with stable CAD may depend on the extent of ischemic myocardium (67,68). Large retrospective data and post hoc analysis of the COURAGE trail, suggested that myocardial revascularization compared with medical therapy had greater survival benefit only in patients with a moderate to large mass of inducible ischemia (>10% myocardium being ischemic), but specific thresholds for HF patients have not been defined yet (67,68). The value of risk stratification for patients with stable CAD seems to be of considerable importance to segregate low-risk patients, who can safely be treated medically from high-risk patients, who may benefit from angiography and potential revascularization (69). This may be particularly true in patients with HF and reduced LVEF, because the risk associated with revascularization procedures, especially for coronary artery bypass grafting, is particularly high in this population. In this context, perfusion CMR may be complementary and additive to DGE viability testing for selecting HF patients for revascularization. However, these concepts need to be further investigated, because no randomized trials addressing the value of different treatment strategies based on perfusion studies have been conducted yet. Furthermore, proving the value of perfusion CMR specifically in HF patients may be challenging considering that these patients may present with multivessel disease and balanced hypoperfusion (70,71) or thinned myocardium due to prior MI, which may cause limitations due to spatial resolution and partial volume effects (typical in-plane spatial resolution of CMR perfusion sequences: 2–3 × 2–3 mm). However, a recent report showed that diagnostic accuracy of perfusion CMR for predicting flow limiting coronary stenoses was high even in segments with subendocardial scar (72).

POTENTIAL APPLICATION OF CMR IN GUIDING INDICATIONS FOR RESYNCHRONIZATION AND INTERNAL CARDIAC DEFIBRILLATOR THERAPY

Cardiac Resynchronization Therapy

CRT has been shown to improve survival and quality of life and reduce hospitalizations in HF patients with reduced LVEF and wide QRS complex (73). Applying current selection criteria for CRT, approximately 30% of the treated patients do not respond to this complex and costly treatment. The current selection of patients is mainly based on symptoms, LVEF, and QRS duration. Small observational and nonrandomized trials have promoted several echocardiographic parameters of mechanical dyssynchrony to select patients for CRT. Unfortunately, larger multicenter trials did not confirm these results, questioning the

role of mechanical dyssynchrony in patient selection for CRT (74). Over the past few years, different CMR methods for the assessment of mechanical dyssynchrony, including myocardial tagging, myocardial- and flow-velocity encoded imaging, have been described (75–79). There is hope, that novel CMR technology will have a superior reproducibility for the assessment of dyssynchrony and, therefore, provide greater accuracy in predicting response to CRT. Recent reports showed promising results using CMR techniques to predict response to CRT (80–82). Moreover, not only the severity of dyssynchrony, but also the amount of scar tissue and the spatial relation of myocardial scar and the site of LV pacing are important for CRT response. Multiple studies have shown, that the global extent of myocardial scar was inversely related to CRT response, especially in case of extensive inferolateral or septal scar (82–84). In this context, the ability of CMR for simultaneous noninvasive visualization of cardiac venous anatomy and myocardial scar tissue may be useful for an optimal planning of the CRT implantation and identification of the ideal cardiac vein for the placement of the LV lead (85). However, further studies are needed to better define the value of CMR for predicting a favorable response to CRT.

Internal Cardiac Defibrillator

Implantation of an Internal Cardiac Defibrillator (ICD) has become the standard of care in patients at highest risk for sudden cardiac death, because several trials demonstrated an impressive reduction in mortality for primary and secondary prophylaxis (4). Because LVEF is the strongest predictor of mortality and sudden cardiac death, the indication for primary prophylactic ICD implantation is mainly based on LVEF, with different cutoff values depending on the cause of HF (4). However, current risk assessment after MI remains suboptimal, and the need for more accurate prognostication for sudden cardiac death is evident (86). Areas of MI are composed of a core zone of scar tissue and a peri-infarct zone. The latter represents the morphological substrate for ventricular re-entry tachycardia after MI and is characterized by a heterogeneous tissue containing both myocardial fibrosis and viable myocardial cells (87,88). Quantitative determination of the peri-infarct zone by CMR is based on DGE images. The core zone of MI is characterized by the highest distribution volume of gadolinium and shows the highest signal intensity on DGE images. Conversely, the peri-infarct zone has an intermediate signal intensity due to an intermediate distribution volume and wash-out kinetic of gadolinium compared to the core zone and the remote (noninfarcted) myocardium. Several studies showed that the size of the peri-infarct zone predicts mortality, arrhythmic events and inducibility of ventricular tachycardia among patients with CAD and reduced LVEF (89–91). In this context, peri-infarct zone quantification may be useful for risk stratification and more targeted ICD implantation after MI. However, this concept needs to be tested in specifically designed trials.

CMR FOR THE ASSESSMENT OF CONSTRICTIVE PERICARDITIS

Constrictive pericarditis (CP) is most frequently the result of a long-standing pericardial inflammation, leading to a reduced pericardial compliance and consequent constriction of the cardiac chambers. Increased cardiac filling pressures with equalization of the end-diastolic pressure of all four chambers and an exaggerated interventricular coupling are pathophysiological consequences of pericardial constriction (92). Bilateral atrial enlargement, dilatation of the inferior vena cava, normal ventricular dimensions and ejection fraction, and thickening of the pericardium are typical morphologic changes, which may raise the suspicion of CP. The differential diagnosis of HF, especially of restrictive CMP, and CP may be challenging, because symptoms, clinical signs, and some of the above-mentioned morphological characteristics may be similar (92,93). The identification of specific hemodynamic features and a thickening of the pericardium are valuable diagnostic clues for differentiating CP from restrictive CMP (92). Typical and almost pathognomonic hemodynamic features of CP consist in augmented ventricular coupling, resulting in increased respiratory variation of the left and right chamber pressures. The assessment of these hemodynamic changes is mostly domain of cardiac catheterization or Doppler echocardiography (94). However, the demonstration of an early diastolic excursion of the interventricular septum toward the LV, which is a direct consequence of augmented ventricular coupling, may be visualized on cine SSFP CMR (95). This phenomenon, called septal "bounce," has a high sensitivity and specificity for CP (95). Recently, the implementation of real-time cine CMR imaging with assessment of the interventricular septal motion during respiratory maneuvers has been suggested as a further expansion of CMR for the functional assessment of CP and as a powerful diagnostic tool for differentiating CP and restrictive CMP (96).

CMR and cardiac-CT have clear advantages compared to echocardiography for the morphological assessment of the pericardium, which is critical for the diagnosis of CP, because pericardial thickness is one of the most important criterion of CP. A pericardial thickness of < 2mm is considered normal, while >4 mm as assessed with black-blood spin-echo imaging is highly specific for CP, in a correct clinical setting (Fig. 9; 97). The pericardium may be visualized with black-blood or bright-blood SSFP cine images, showing a low signal intensity on both sequences. Additionally, tagging sequences may be used to visualize the adhesion between the visceral and parietal pericardium, resulting in reduced or absence of relative motion between the two layers (98). Therefore, CMR has the ability to integrate extensive functional and morphological assessment of the pericardium and has become an attractive diagnostic tool for CP.

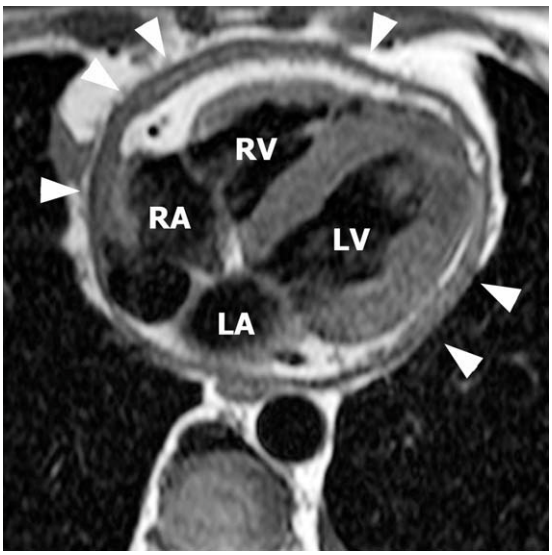

Figure 9. Constrictive pericarditis. T1-weighted double inversion spin echo axial image showing a diffuse and extensive thickening of the pericardium (arrowhead), consistent with constrictive pericarditis. LV, left ventricle; RV, right ventricle; LA, left atrium; RA, right atrium.

LIMITATION OF CMR: PATIENTS WITH CARDIAC DEVICES AND RENAL FAILURE FOR CONTRAST IMAGING

Permanent Pacemakers or Internal Cardiac Defibrillator Recipients

A significant proportion of HF patients have permanent pacemakers or ICDs. Because both magnetic fields and radiofrequency may cause potential movement, programming changes, and heating of the device, there are serious concerns for performing CMR in devices' recipients (99–101). However, several case series have reported the safety of CMR in pacemaker and ICD recipients, but changes in battery voltages, lead thresholds, and device programming may occur (102,103). In this context, the decision whether to perform a CMR should be decided on an individual basis depending on the specific ratio of risks and benefits. A safety protocol requiring a collaboration of electrophysiologist and cardiac imager has been proposed to minimize risks of CMR at 1.5 Tesla in cardiac device recipients (104).

Renal Insufficiency: A Limitation for Gadolinium Use

The use of gadolinium has been related to nephrogenic systemic fibrosis (NSF) in patients with renal failure, which is a frequent comorbidity in HF patients. The pathophysiology of NSF is not fully understood, but the accumulation of gadolinium in tissues and organs, with consequent toxic effect leading to fibrosis and organ failure has been postulated (105). The mortality of NSF is high, and no specific treatment is available. So far, NSF has been observed only in patients with severe renal failure, defined as a creatinine clearance < 30 mL/min/1.73 m^2, since the elimination of gadolinium, which has mainly a renal clearance, is substantially prolonged in such patients. In a general population referred for contrast MRI, the incidence of NSF is estimated between 0.04% and 0.001%, but may rise up to 2.4% in dialysis dependent patients (106,107). The use of gadodiamide gadolinium compounds, repeated gadolinium exposure, concomitant administration of iron therapy, and higher total dosages are risk factors of NSF (105). Therefore, renal function should be determined by laboratory tests before administration of gadolinium, and contrast-free CMR should be preferred whenever possible in patients with severe renal failure. Noteworthy, gadolinium compounds are not FDA approved for cardiac imaging and are, therefore, used with an off-label indication.

CONCLUSION

CMR has become an important tool for diagnosis, risk stratification, and therapeutic guidance of patients with HF. The capabilities of this imaging technique are supported by a robust and extensive literature. CMR is now a mature technique, ready for widespread use in clinical practice. Its versatility and accuracy in defining cardiac function and volumetrics; myocardial perfusion; and myocardial tissue characterization are the major advantages compared to other imaging techniques.

ACKNOWLEDGMENT

S.M. is funded by the Swiss National Science Foundation, Berne, Switzerland.

REFERENCES

1. Bonow RO, Carabello BA, Chatterjee K, et al. 2008 focused update incorporated into the ACC/AHA 2006 guidelines for the management of patients with valvular heart disease: a report of the American College of Cardiology/American Heart Association Task Force on Practice Guidelines (Writing Committee to revise the 1998 guidelines for the management of patients with valvular heart disease). Endorsed by the Society of Cardiovascular Anesthesiologists, Society for Cardiovascular Angiography and Interventions, and Society of Thoracic Surgeons. J Am Coll Cardiol 2008;52:e1–142.
2. Remme WJ, Swedberg K. Guidelines for the diagnosis and treatment of chronic heart failure. Eur Heart J 2001;22:1527–1560.
3. Vardas PE, Auricchio A, Blanc JJ, et al. Guidelines for cardiac pacing and cardiac resynchronization therapy: The Task Force for Cardiac Pacing and Cardiac Resynchronization Therapy of the European Society of Cardiology. Developed in collaboration with the European Heart Rhythm Association. Eur Heart J 2007;28:2256–2295.
4. Zipes DP, Camm AJ, Borggrefe M, et al. ACC/AHA/ESC 2006 guidelines for management of patients with ventricular arrhythmias and the prevention of sudden cardiac death--executive summary: A report of the American College of Cardiology/American Heart Association Task Force and the European Society of Cardiology Committee for Practice Guidelines (Writing Committee to Develop Guidelines for Management of Patients with Ventricular Arrhythmias and the Prevention of Sudden Cardiac Death) Developed in collaboration with the European Heart Rhythm Association and the Heart Rhythm Society. Eur Heart J 2006;27:2099–2140.
5. de Groote P, Millaire A, Foucher-Hossein C, et al. Right ventricular ejection fraction is an independent predictor of survival in

patients with moderate heart failure. J Am Coll Cardiol 1998; 32:948–954.
6. Ghio S, Gavazzi A, Campana C, et al. Independent and additive prognostic value of right ventricular systolic function and pulmonary artery pressure in patients with chronic heart failure. J Am Coll Cardiol 2001;37:183–188.
7. Barkhausen J, Ruehm SG, Goyen M, Buck T, Laub G, Debatin JF. MR evaluation of ventricular function: true fast imaging with steady-state precession versus fast low-angle shot cine MR imaging: feasibility study. Radiology 2001;219:264–269.
8. Thiele H, Nagel E, Paetsch I, et al. Functional cardiac MR imaging with steady-state free precession (SSFP) significantly improves endocardial border delineation without contrast agents. J Magn Reson Imaging 2001;14:362–367.
9. Danilouchkine MG, Westenberg JJ, de Roos A, Reiber JH, Lelieveldt BP. Operator induced variability in cardiovascular MR: left ventricular measurements and their reproducibility. J Cardiovasc Magn Reson 2005;7:447–457.
10. Maceira AM, Prasad SK, Khan M, Pennell DJ. Normalized left ventricular systolic and diastolic function by steady state free precession cardiovascular magnetic resonance. J Cardiovasc Magn Reson 2006;8:417–426.
11. Maceira AM, Prasad SK, Khan M, Pennell DJ. Reference right ventricular systolic and diastolic function normalized to age, gender and body surface area from steady-state free precession cardiovascular magnetic resonance. Eur Heart J 2006;27: 2879–2888.
12. Paulus WJ, Tschope C, Sanderson JE, et al. How to diagnose diastolic heart failure: a consensus statement on the diagnosis of heart failure with normal left ventricular ejection fraction by the Heart Failure and Echocardiography Associations of the European Society of Cardiology. Eur Heart J 2007;28:2539–2550.
13. Bhatia RS, Tu JV, Lee DS, et al. Outcome of heart failure with preserved ejection fraction in a population-based study. N Engl J Med 2006;355:260–269.
14. Hansen A, Haass M, Zugck C, et al. Prognostic value of Doppler echocardiographic mitral inflow patterns: implications for risk stratification in patients with chronic congestive heart failure. J Am Coll Cardiol 2001;37:1049–1055.
15. Paelinck BP, de Roos A, Bax JJ, et al. Feasibility of tissue magnetic resonance imaging: a pilot study in comparison with tissue Doppler imaging and invasive measurement. J Am Coll Cardiol 2005;45:1109–1116.
16. Rathi VK, Doyle M, Yamrozik J, et al. Routine evaluation of left ventricular diastolic function by cardiovascular magnetic resonance: a practical approach. J Cardiovasc Magn Reson 2008; 10:36.
17. Nagel E, Stuber M, Burkhard B, et al. Cardiac rotation and relaxation in patients with aortic valve stenosis. Eur Heart J 2000;21:582–589.
18. Suzuki J, Caputo GR, Masui T, Chang JM, O'Sullivan M, Higgins CB. Assessment of right ventricular diastolic and systolic function in patients with dilated cardiomyopathy using cine magnetic resonance imaging. Am Heart J 1991;122:1035–1040.
19. Bardy GH, Lee KL, Mark DB, et al. Amiodarone or an implantable cardioverter-defibrillator for congestive heart failure. N Engl J Med 2005;352:225–237.
20. Maron BJ, Towbin JA, Thiene G, et al. Contemporary definitions and classification of the cardiomyopathies: an American Heart Association Scientific Statement from the Council on Clinical Cardiology, Heart Failure and Transplantation Committee; Quality of Care and Outcomes Research and Functional Genomics and Translational Biology Interdisciplinary Working Groups; and Council on Epidemiology and Prevention. Circulation 2006;113:1807–1816.
21. Mahrholdt H, Wagner A, Judd RM, Sechtem U, Kim RJ. Delayed enhancement cardiovascular magnetic resonance assessment of non-ischaemic cardiomyopathies. Eur Heart J 2005;26: 1461–1474.
22. Deugnier Y, Brissot P, Loreal O. Iron and the liver: update 2008. J Hepatol 2008;48 Suppl 1:S113–S123.
23. Zurlo MG, De Stefano P, Borgna-Pignatti C, et al. Survival and causes of death in thalassaemia major. Lancet 1989;2:27–30.
24. Wesbey GE, Higgins CB, McNamara MT, et al. Effect of gadolinium-DTPA on the magnetic relaxation times of normal and infarcted myocardium. Radiology 1984;153:165–169.
25. Rehwald WG, Fieno DS, Chen EL, Kim RJ, Judd RM. Myocardial magnetic resonance imaging contrast agent concentrations after reversible and irreversible ischemic injury. Circulation 2002; 105:224–229.
26. Kim RJ, Chen EL, Lima JA, Judd RM. Myocardial Gd-DTPA kinetics determine MRI contrast enhancement and reflect the extent and severity of myocardial injury after acute reperfused infarction. Circulation 1996;94:3318–3326.
27. Kim RJ, Fieno DS, Parrish TB, et al. Relationship of MRI delayed contrast enhancement to irreversible injury, infarct age, and contractile function. Circulation 1999;100:1992–2002.
28. Simonetti OP, Kim RJ, Fieno DS, et al. An improved MR imaging technique for the visualization of myocardial infarction. Radiology 2001;218:215–223.
29. Kellman P, Arai AE, McVeigh ER, Aletras AH. Phase-sensitive inversion recovery for detecting myocardial infarction using gadolinium-delayed hyperenhancement. Magn Reson Med 2002;47: 372–383.
30. He T, Gatehouse PD, Kirk P, et al. Black-blood T2* technique for myocardial iron measurement in thalassemia. J Magn Reson Imaging 2007;25:1205–1209.
31. Simonetti OP, Finn JP, White RD, Laub G, Henry DA. "Black blood" T2-weighted inversion-recovery MR imaging of the heart. Radiology 1996;199:49–57.
32. Aletras AH, Kellman P, Derbyshire JA, Arai AE. ACUT2E TSE-SSFP: a hybrid method for T2-weighted imaging of edema in the heart. Magn Reson Med 2008;59:229–235.
33. Braunwald E, Rutherford JD. Reversible ischemic left ventricular dysfunction: evidence for the "hibernating myocardium". J Am Coll Cardiol 1986;8:1467–1470.
34. Kloner RA, Jennings RB. Consequences of brief ischemia: stunning, preconditioning, and their clinical implications: part 1. Circulation 2001;104:2981–2989.
35. Dorn GWn. Novel pharmacotherapies to abrogate postinfarction ventricular remodeling. Nat Rev Cardiol 2009;6:283–291.
36. Maceira AM, Joshi J, Prasad SK, et al. Cardiovascular magnetic resonance in cardiac amyloidosis. Circulation 2005;111:186–193.
37. Moon JC, McKenna WJ, McCrohon JA, Elliott PM, Smith GC, Pennell DJ. Toward clinical risk assessment in hypertrophic cardiomyopathy with gadolinium cardiovascular magnetic resonance. J Am Coll Cardiol 2003;41:1561–1567.
38. Moon JC, Sachdev B, Elkington AG, et al. Gadolinium enhanced cardiovascular magnetic resonance in Anderson-Fabry disease. Evidence for a disease specific abnormality of the myocardial interstitium. Eur Heart J 2003;24:2151–2155.
39. Patel MR, Cawley PJ, Heitner JF, et al. Detection of myocardial damage in patients with sarcoidosis. Circulation 2009;120: 1969–1977
40. McCrohon JA, Moon JC, Prasad SK, et al. Differentiation of heart failure related to dilated cardiomyopathy and coronary artery disease using gadolinium-enhanced cardiovascular magnetic resonance. Circulation 2003;108:54–59.
41. Casolo G, Minneci S, Manta R, et al. Identification of the ischemic etiology of heart failure by cardiovascular magnetic resonance imaging: diagnostic accuracy of late gadolinium enhancement. Am Heart J 2006;151:101–108.
42. Soriano CJ, Ridocci F, Estornell J, Jimenez J, Martinez V, De Velasco JA. Noninvasive diagnosis of coronary artery disease in patients with heart failure and systolic dysfunction of uncertain etiology, using late gadolinium-enhanced cardiovascular magnetic resonance. J Am Coll Cardiol 2005;45:743–748.
43. Soriano CJ, Ridocci F, Estornell J, et al. Late gadolinium-enhanced cardiovascular magnetic resonance identifies patients with standardized definition of ischemic cardiomyopathy: a single centre experience. Int J Cardiol 2007;116:167–173.
44. Anderson LJ, Holden S, Davis B, et al. Cardiovascular T2-star (T2*) magnetic resonance for the early diagnosis of myocardial iron overload. Eur Heart J 2001;22:2171–2179.
45. Anderson LJ, Wonke B, Prescott E, Holden S, Walker JM, Pennell DJ. Comparison of effects of oral deferiprone and subcutaneous desferrioxamine on myocardial iron concentrations and ventricular function in beta-thalassaemia. Lancet 2002;360: 516–520.
46. Kirk P, Roughton M, Porter JB, et al. Cardiac T2* magnetic resonance for prediction of cardiac complications in thalassemia major. Circulation 2009;120:1961–1968.

47. Abdel-Aty H, Boye P, Zagrosek A, et al. Diagnostic performance of cardiovascular magnetic resonance in patients with suspected acute myocarditis: comparison of different approaches. J Am Coll Cardiol 2005;45:1815–1822.
48. Marie PY, Angioi M, Carteaux JP, et al. Detection and prediction of acute heart transplant rejection with the myocardial T2 determination provided by a black-blood magnetic resonance imaging sequence. J Am Coll Cardiol 2001;37:825–831.
49. Taylor AJ, Vaddadi G, Pfluger H, et al. Diagnostic performance of multisequential cardiac magnetic resonance imaging in acute cardiac allograft rejection. Eur J Heart Fail 2010;12:45–51.
50. Wagner A, Mahrholdt H, Holly TA, et al. Contrast-enhanced MRI and routine single photon emission computed tomography (SPECT) perfusion imaging for detection of subendocardial myocardial infarcts: an imaging study. Lancet 2003;361:374–379.
51. Allman KC, Shaw LJ, Hachamovitch R, Udelson JE. Myocardial viability testing and impact of revascularization on prognosis in patients with coronary artery disease and left ventricular dysfunction: a meta-analysis. J Am Coll Cardiol 2002;39:1151–1158.
52. Underwood SR, Bax JJ, vom Dahl J, et al. Imaging techniques for the assessment of myocardial hibernation. Report of a Study Group of the European Society of Cardiology. Eur Heart J 2004; 25:815–836.
53. Beek AM, Kuhl HP, Bondarenko O, et al. Delayed contrast-enhanced magnetic resonance imaging for the prediction of regional functional improvement after acute myocardial infarction. J Am Coll Cardiol 2003;42:895–901.
54. Choi KM, Kim RJ, Gubernikoff G, Vargas JD, Parker M, Judd RM. Transmural extent of acute myocardial infarction predicts long-term improvement in contractile function. Circulation 2001;104:1101–1107.
55. Kim RJ, Wu E, Rafael A, et al. The use of contrast-enhanced magnetic resonance imaging to identify reversible myocardial dysfunction. N Engl J Med 2000;343:1445–1453.
56. Selvanayagam JB, Kardos A, Francis JM, et al. Value of delayed-enhancement cardiovascular magnetic resonance imaging in predicting myocardial viability after surgical revascularization. Circulation 2004;110:1535–1541.
57. Ichikawa Y, Sakuma H, Suzawa N, et al. Late gadolinium-enhanced magnetic resonance imaging in acute and chronic myocardial infarction. Improved prediction of regional myocardial contraction in the chronic state by measuring thickness of nonenhanced myocardium. J Am Coll Cardiol 2005;45: 901–909.
58. Knuesel PR, Nanz D, Wyss C, et al. Characterization of dysfunctional myocardium by positron emission tomography and magnetic resonance: relation to functional outcome after revascularization. Circulation 2003;108:1095–1100.
59. Bekkers SC, Yazdani SK, Virmani R, Waltenberger J. Microvascular obstruction: underlying pathophysiology and clinical diagnosis. J Am Coll Cardiol 2010;55:1649–1660.
60. Nijveldt R, Hofman MB, Hirsch A, et al. Assessment of microvascular obstruction and prediction of short-term remodeling after acute myocardial infarction: cardiac MR imaging study. Radiology 2009;250:363–370.
61. Nijveldt R, Beek AM, Hirsch A, et al. Functional recovery after acute myocardial infarction: comparison between angiography, electrocardiography, and cardiovascular magnetic resonance measures of microvascular injury. J Am Coll Cardiol 2008;52: 181–189.
62. Wu KC, Zerhouni EA, Judd RM, et al. Prognostic significance of microvascular obstruction by magnetic resonance imaging in patients with acute myocardial infarction. Circulation 1998;97: 765–772.
63. Wellnhofer E, Olariu A, Klein C, et al. Magnetic resonance low-dose dobutamine test is superior to SCAR quantification for the prediction of functional recovery. Circulation 2004;109: 2172–2174.
64. Nandalur KR, Dwamena BA, Choudhri AF, Nandalur MR, Carlos RC. Diagnostic performance of stress cardiac magnetic resonance imaging in the detection of coronary artery disease: a meta-analysis. J Am Coll Cardiol 2007;50:1343–1353.
65. Schwitter J, Nanz D, Kneifel S, et al. Assessment of myocardial perfusion in coronary artery disease by magnetic resonance: a comparison with positron emission tomography and coronary angiography. Circulation 2001;103:2230–2235.
66. Schwitter J, Wacker CM, van Rossum AC, et al. MR-IMPACT: comparison of perfusion-cardiac magnetic resonance with single-photon emission computed tomography for the detection of coronary artery disease in a multicentre, multivendor, randomized trial. Eur Heart J 2008;29:480–489.
67. Hachamovitch R, Hayes SW, Friedman JD, Cohen I, Berman DS. Comparison of the short-term survival benefit associated with revascularization compared with medical therapy in patients with no prior coronary artery disease undergoing stress myocardial perfusion single photon emission computed tomography. Circulation 2003;107:2900–2907.
68. Shaw LJ, Berman DS, Maron DJ, et al. Optimal medical therapy with or without percutaneous coronary intervention to reduce ischemic burden: results from the Clinical Outcomes Utilizing Revascularization and Aggressive Drug Evaluation (COURAGE) trial nuclear substudy. Circulation 2008;117:1283–1291.
69. Gibbons RJ, Abrams J, Chatterjee K, et al. ACC/AHA 2002 guideline update for the management of patients with chronic stable angina--summary article: a report of the American College of Cardiology/American Heart Association Task Force on Practice Guidelines (Committee on the Management of Patients With Chronic Stable Angina). Circulation 2003;107:149–158.
70. Lima RS, Watson DD, Goode AR, et al. Incremental value of combined perfusion and function over perfusion alone by gated SPECT myocardial perfusion imaging for detection of severe three-vessel coronary artery disease. J Am Coll Cardiol 2003;42: 64–70.
71. Ragosta M, Bishop AH, Lipson LC, et al. Comparison between angiography and fractional flow reserve versus single-photon emission computed tomographic myocardial perfusion imaging for determining lesion significance in patients with multivessel coronary disease. Am J Cardiol 2007;99:896–902.
72. Klein C, Nagel E, Gebker R, et al. Magnetic resonance adenosine perfusion imaging in patients after coronary artery bypass graft surgery. JACC Cardiovasc Imaging 2009;2:437–445.
73. Cleland JG, Daubert JC, Erdmann E, et al. The effect of cardiac resynchronization on morbidity and mortality in heart failure. N Engl J Med 2005;352:1539–1549.
74. Hawkins NM, Petrie MC, Burgess MI, McMurray JJ. Selecting patients for cardiac resynchronization therapy: the fallacy of echocardiographic dyssynchrony. J Am Coll Cardiol 2009;53: 1944–1959.
75. Koos R, Neizel M, Schummers G, et al. Feasibility and initial experience of assessment of mechanical dyssynchrony using cardiovascular magnetic resonance and semi-automatic border detection. J Cardiovasc Magn Reson 2008;10:49.
76. Lardo AC, Abraham TP, Kass DA. Magnetic resonance imaging assessment of ventricular dyssynchrony: current and emerging concepts. J Am Coll Cardiol 2005;46:2223–2228.
77. Marsan NA, Westenberg JJ, Tops LF, et al. Comparison between tissue Doppler imaging and velocity-encoded magnetic resonance imaging for measurement of myocardial velocities, assessment of left ventricular dyssynchrony, and estimation of left ventricular filling pressures in patients with ischemic cardiomyopathy. Am J Cardiol 2008;102:1366–1372.
78. Muellerleile K, Baholli L, Groth M, et al. Interventricular mechanical dyssynchrony: quantification with velocity-encoded MR imaging. Radiology 2009;253:364–371.
79. Rutz AK, Manka R, Kozerke S, Roas S, Boesiger P, Schwitter J. Left ventricular dyssynchrony in patients with left bundle branch block and patients after myocardial infarction: integration of mechanics and viability by cardiac magnetic resonance. Eur Heart J 2009;30:2117–2127.
80. Bilchick KC, Dimaano V, Wu KC, et al. Cardiac magnetic resonance assessment of dyssynchrony and myocardial scar predicts function class improvement following cardiac resynchronization therapy. JACC Cardiovasc Imaging 2008;1:561–568.
81. Chalil S, Stegemann B, Muhyaldeen S, et al. Intraventricular dyssynchrony predicts mortality and morbidity after cardiac resynchronization therapy: a study using cardiovascular magnetic resonance tissue synchronization imaging. J Am Coll Cardiol 2007;50:243–252.
82. Marsan NA, Westenberg JJ, Ypenburg C, et al. Magnetic resonance imaging and response to cardiac resynchronization therapy: relative merits of left ventricular dyssynchrony and scar tissue. Eur Heart J 2009;30:2360–2367.

83. Bleeker GB, Kaandorp TA, Lamb HJ, et al. Effect of posterolateral scar tissue on clinical and echocardiographic improvement after cardiac resynchronization therapy. Circulation 2006;113: 969–976.
84. White JA, Yee R, Yuan X, et al. Delayed enhancement magnetic resonance imaging predicts response to cardiac resynchronization therapy in patients with intraventricular dyssynchrony. J Am Coll Cardiol 2006;48:1953–1960.
85. Younger JF, Plein S, Crean A, Ball SG, Greenwood JP. Visualization of coronary venous anatomy by cardiovascular magnetic resonance. J Cardiovasc Magn Reson 2009;11:26.
86. Buxton AE. Risk stratification for sudden death: do we need anything more than ejection fraction? Card Electrophysiol Rev 2003;7:434–437.
87. Ursell PC, Gardner PI, Albala A, Fenoglio JJJ, Wit AL. Structural and electrophysiological changes in the epicardial border zone of canine myocardial infarcts during infarct healing. Circ Res 1985;56:436–451.
88. Yao JA, Hussain W, Patel P, Peters NS, Boyden PA, Wit AL. Remodeling of gap junctional channel function in epicardial border zone of healing canine infarcts. Circ Res 2003;92: 437–443.
89. Roes SD, Borleffs CJ, van der Geest RJ, et al. Infarct tissue heterogeneity assessed with contrast-enhanced MRI predicts spontaneous ventricular arrhythmia in patients with ischemic cardiomyopathy and implantable cardioverter-defibrillator. Circ Cardiovasc Imaging 2009;2:183–190.
90. Schmidt A, Azevedo CF, Cheng A, et al. Infarct tissue heterogeneity by magnetic resonance imaging identifies enhanced cardiac arrhythmia susceptibility in patients with left ventricular dysfunction. Circulation 2007;115:2006–2014.
91. Yan AT, Shayne AJ, Brown KA, et al. Characterization of the peri-infarct zone by contrast-enhanced cardiac magnetic resonance imaging is a powerful predictor of post-myocardial infarction mortality. Circulation 2006;114:32–39.
92. Little WC, Freeman GL. Pericardial disease. Circulation 2006; 113:1622–1632.
93. Nishimura RA. Constrictive pericarditis in the modern era: a diagnostic dilemma. Heart 2001;86:619–623.
94. Hurrell DG, Nishimura RA, Higano ST, et al. Value of dynamic respiratory changes in left and right ventricular pressures for the diagnosis of constrictive pericarditis. Circulation 1996;93: 2007–2913.
95. Giorgi B, Mollet NR, Dymarkowski S, Rademakers FE, Bogaert J. Clinically suspected constrictive pericarditis: MR imaging assessment of ventricular septal motion and configuration in patients and healthy subjects. Radiology 2003;228:417–424.
96. Francone M, Dymarkowski S, Kalantzi M, Rademakers FE, Bogaert J. Assessment of ventricular coupling with real-time cine MRI and its value to differentiate constrictive pericarditis from restrictive cardiomyopathy. Eur Radiol 2006;16:944–951.
97. Masui T, Finck S, Higgins CB. Constrictive pericarditis and restrictive cardiomyopathy: evaluation with MR imaging. Radiology 1992;182:369–373.
98. Kojima S, Yamada N, Goto Y. Diagnosis of constrictive pericarditis by tagged cine magnetic resonance imaging. N Engl J Med 1999;341:373–374.
99. Erlebacher JA, Cahill PT, Pannizzo F, Knowles RJ. Effect of magnetic resonance imaging on DDD pacemakers. Am J Cardiol 1986;57:437–440.
100. Hayes DL, Holmes DRJ, Gray JE. Effect of 1.5 Tesla nuclear magnetic resonance imaging scanner on implanted permanent pacemakers. J Am Coll Cardiol 1987;10:782–786.
101. Shellock FG, Tkach JA, Ruggieri PM, Masaryk TJ. Cardiac pacemakers, ICDs, and loop recorder: evaluation of translational attraction using conventional ("long-bore") and "short-bore" 1.5- and 3.0-Tesla MR systems. J Cardiovasc Magn Reson 2003;5: 387–397.
102. Gimbel JR, Kanal E, Schwartz KM, Wilkoff BL. Outcome of magnetic resonance imaging (MRI) in selected patients with implantable cardioverter defibrillators (ICDs). Pacing Clin Electrophysiol 2005;28:270–273.
103. Martin ET, Coman JA, Shellock FG, Pulling CC, Fair R, Jenkins K. Magnetic resonance imaging and cardiac pacemaker safety at 1.5-Tesla. J Am Coll Cardiol 2004;43:1315–3124.
104. Nazarian S, Roguin A, Zviman MM, et al. Clinical utility and safety of a protocol for noncardiac and cardiac magnetic resonance imaging of patients with permanent pacemakers and implantable-cardioverter defibrillators at 1.5 Tesla. Circulation 2006;114:1277–1284.
105. Kribben A, Witzke O, Hillen U, Barkhausen J, Daul AE, Erbel R. Nephrogenic systemic fibrosis: pathogenesis, diagnosis, and therapy. J Am Coll Cardiol 2009;53:1621–18.
106. Deo A, Fogel M, Cowper SE. Nephrogenic systemic fibrosis: a population study examining the relationship of disease development to gadolinium exposure. Clin J Am Soc Nephrol 2007;2: 264–267.
107. Wertman R, Altun E, Martin DR, et al. Risk of nephrogenic systemic fibrosis: evaluation of gadolinium chelate contrast agents at four American universities. Radiology 2008;248:799–806.